

## Quantum Saturation of a Bose Gas: Excitons in Cu<sub>2</sub>O

D. Snoke and J. P. Wolfe

*Physics Department and Materials Research Laboratory, University of Illinois at Urbana-Champaign, Urbana, Illinois 61801*

and

A. Mysyrowicz

*Group de Physique des Solides, Ecole Normale Supérieure, Université de Paris VII, F-75 005 Paris, France*

(Received 6 April 1987)

Quantum statistics of an ideal gas of Bose particles predicts a phase boundary for Bose-Einstein condensation. The expected relation for the saturated-gas density,  $n = CT^{3/2}$ , is observed for an exciton gas in Cu<sub>2</sub>O by time resolution of the energy spectrum.

PACS numbers: 71.35.+z, 05.30.-d, 67.90.+z, 78.47.+p

More than sixty years after Einstein originally considered the case of an ideal gas of noninteracting Bose particles,<sup>1</sup> experimental verification of its quantum-statistical properties remains a challenging task. In such a system, consisting of free particles with integral spin, Bose-Einstein (BE) statistics requires an excited-state occupation number of the form  $f(E, \mu, T) = \{\exp[(E - \mu)/k_B T] - 1\}^{-1}$ , where  $E$  is the single-particle kinetic energy and  $T$  is the gas temperature. The chemical potential  $\mu$  is determined by the condition  $N = \int_0^\infty f(E, \mu, T) D(E) \times dE$ , where  $N$  is the number of particles in excited states in volume  $V$ , and  $D(E) \propto VE^{1/2}$  is the density of states.  $\mu$  is large and negative at low density, and approaches zero as the number of particles is increased. At a given  $T$  and  $V$  the number of particles in excited states cannot exceed a certain critical value, because the above integral is finite even at  $\mu = 0$ , the maximum allowable value. The critical density for this excited-state saturation at  $\mu = 0$  is given by

$$n_c = N_c/V = 2.612g(m/2\pi\hbar^2)^{3/2}(k_B T)^{3/2} = CT^{3/2}, \quad (1)$$

where  $m$  is the particle mass and  $g$  is the spin degeneracy. According to Einstein, once the population of the excited states reaches this saturation condition, further addition of particles at constant  $T$  and  $V$  must be accommodated by the ground state—Bose-Einstein condensation (BEC).

For some time it has been recognized that excitons in semiconductors may provide a test of BE quantum statistics.<sup>2-4</sup> The exciton, or bound electron-hole pair, has several desirable properties: (1) Its mass is much smaller than that of an atom or molecule, thus requiring much lower  $n_c$  for a given  $T$ ; (2) the excitonic-gas density can be controlled over a wide range by changing optical-excitation level; and (3) in many cases the excitonic gas emits a recombination luminescence which directly reflects the kinetic-energy distribution in the gas. Degenerate BE statistics have been reported for excitons in Ge<sup>5</sup> and biexcitons in CuCl.<sup>6</sup> In the latter case, a stable

macroscopic occupation of low-energy states was observed by resonant pumping of these states above a critical threshold in excitation power.

One of the most promising systems for the study of an ideal Bose gas involves excitons in Cu<sub>2</sub>O.<sup>2</sup> Hulin, Mysyrowicz, and Benoît à la Guillaume<sup>7</sup> have reported a gradual transition from classical to degenerate Bose statistics for orthoexcitons in Cu<sub>2</sub>O generated by a non-resonant laser, on the basis of a spectral analysis of the time-integrated luminescence from these excitons. With increasing laser intensity, both particle density and temperature of the excitonic gas increased, and the system appeared to approach  $n_c(T)$  asymptotically.

In this Letter, we report a study of *time- and space-resolved* luminescence of orthoexcitons in Cu<sub>2</sub>O. This technique provides direct information about the kinetics of the thermodynamic parameters entering expression (1), namely the exciton temperature  $T$ , the total number  $N$  of excitons in excited states, and the volume  $V$  they occupy inside the crystal. Large variations of these quantities are observed on a nanosecond time scale. However, the ratio  $n/n_c$  remains constant, near unity, during most of the excitation. We believe that this represents the first experimental verification of quantum saturation, a concept central to Bose statistics and condensation. The observed saturation condition,  $n = CT^{3/2}$ , is verified over an order of magnitude of density.

Our experiments use high-purity naturally grown crystals of Cu<sub>2</sub>O which are immersed in superfluid helium and excited by a cavity-dumped Ar<sup>+</sup> laser ( $\lambda = 5145 \text{ \AA}$ , pulse width = 10 ns, pulse energy  $\leq 1 \mu\text{J}$ ). The laser photons produce electron-hole pairs with large kinetic energies ( $h\nu - E_{\text{gap}} \approx 0.375 \text{ eV}$ ), which thermalize by emission of optical phonons and pair into excitons (binding energy  $\approx 0.15 \text{ eV}$ , Bohr radius  $\approx 7 \text{ \AA}$ ) on a sub-nanosecond time scale.<sup>8</sup> The laser beam is focused to a spot as small as  $30 \mu\text{m}$  in diameter on a [100] surface, producing up to  $10^7 \text{ W/cm}^2$  absorbed power. A  $5\times$ -magnified image of the crystal is focused onto the entrance slit of a 1-m spectrometer with typical spectral resolution  $0.25 \text{ \AA}$ . A spatial profile of the luminescence

with about 20- $\mu\text{m}$  resolution is achieved by scanning of the crystal image across a 100- $\mu\text{m}$  entrance slit. Photon-counting detection allows a time-resolved analysis with 1-ns resolution.

Figure 1 shows time-resolved luminescence spectra from  $\text{Cu}_2\text{O}$  at a  $^4\text{He}$  bath temperature of  $T=2\text{ K}$ . In this experiment the image of the excitation region is centered on the spectrometer slit. The solid circles represent the energy distribution function of a homogeneous ideal Bose gas,  $N(E)=f(E,\mu,T)D(E)$ , with values of chemical potential  $\mu$  and temperature  $T$  adjusted for best fits. Because of the unavoidable spatial integration of luminescence along the viewing direction, the best-fit values— $\bar{\mu}$  and  $\bar{T}$ —represent averages over the sample volume.<sup>9</sup> For any reasonable density distribution, the local values of  $\mu$  and  $T$  close to the surface are actually higher than  $\bar{\mu}$  and  $\bar{T}$ . The spectra obtained under these strong excitation conditions are indicative of a highly degenerate gas of excitons with  $\bar{\mu} \approx -0.1k_B\bar{T}$ . Using the exciton mass  $m=2.7m_0$  measured by Caswell, Weiner, and Yu<sup>8</sup> and the above integral for  $N/V$ , we calculate the particle density from the fitted values of  $\bar{\mu}$  and  $\bar{T}$ . The time variation of  $\bar{n}$  and  $\bar{T}$  is plotted in Fig. 2.

Both the gas density and temperature vary substantially during and after the laser pulse. The ratio  $\bar{\mu}/k_B\bar{T}$ , however, remains constant over a wide range of  $\bar{n}$  and  $\bar{T}$  as shown in Fig. 2(c). This is equivalent to noting that

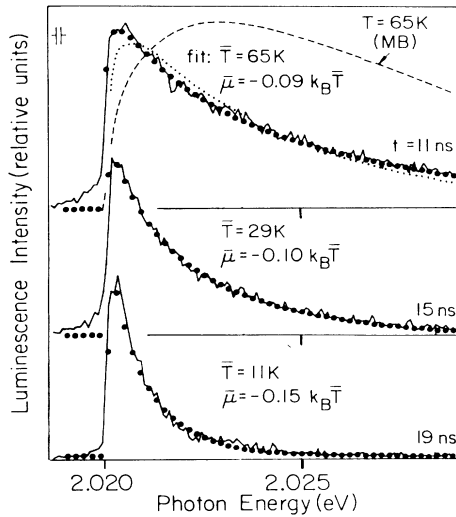


FIG. 1. Time-resolved spectra of the orthoexciton phonon-assisted luminescence in  $\text{Cu}_2\text{O}$  showing quantum-statistical nature of this gas. Maximum absorbed power  $\approx 5 \times 10^6 \text{ W/cm}^2$ . Spectra are collected from the center of the excitation spot, integrated over a 1-ns time interval, and normalized to the same heights. Solid circles indicate best fits for a constant-potential Bose-Einstein distribution. The dotted line is a least-squares fit to the first spectrum, imposing a lower degeneracy  $\mu = -0.3k_B T$ . (The corresponding  $T$  is 43 K.) The dashed curve is a classical ( $\mu < -2k_B T$ ) distribution for the same  $T$  as the first spectrum.

the *shape* of the distribution remains the same during this time interval, except for a change in energy scale. A plot of the fit density versus fit temperature is given in Fig. 3. As the gas density increases and decreases in time, the excitonic temperature also increases and decreases in precisely such a way as to fulfill the condition  $n=CT^{3/2}$ . At the latest times the temperature approaches 5 K as the density decreases, and the spectra change shape to a classical distribution. Although the excitonic-gas temperature rises to very high levels, here up to 70 K, the lattice temperature appears to remain below about 15 K, as indicated by the almost negligible band-gap shift of these spectra. [Compare to the shift of the cw spectra in Fig. 4(a)].

To check the densities derived from the spectroscopic data, we have determined the volume of the exciton gas by measuring luminescence profiles parallel and perpendicular to the surface [inset, Fig. 2(d)]. The time dependence of the gas volume is shown in Fig. 2(d). Figure 2(d) includes the integrated intensity  $I$  divided by this measured volume  $V$ . The relative variation in particle density measured in this way agrees very well (for over 2 orders of magnitude) with that derived from the spectra. Also, the fit densities are within a factor of 2 of the absolute calibration provided by estimates of the excitonic lifetimes and the optical generation rate, on the assumption of unity photon-to-exciton production efficiency.

The quantum degeneracy of the excitonic gas can also be verified without relying on a spectral line-shape analysis. We note that orthoexcitons recombine radiatively via two principal channels: a *phonon-assisted* process, corresponding to the emission line of Fig. 1, and a *direct* process by quadrupole emission. This latter process produces a sharp luminescence line which samples only excitons with near-zero wave vector, namely at  $k_{\text{exciton}}=k_{\text{photon}}$ . Both lines are shown in Fig. 4(a) for a low-density cw-excited exciton gas. The ratio of the peak intensities,  $S_d/S_p$ , should depend on the particle statistics. Specifically, for classical statistics,

$$\frac{S_d}{S_p} = \frac{E_d^{1/2} \exp(-E_d/k_B T)}{E_{\text{max}}^{1/2} \exp(-E_{\text{max}}/k_B T)},$$

where  $E_d = \hbar^2 k_p^2 / 2m \ll k_B T$  and  $E_{\text{max}} = k_B T / 2$  is the energy at the peak of the classical distribution. Thus, for a classical gas, one expects  $S_d/S_p \propto T^{-1/2}$ , independent of  $n$ . Figure 4(b) shows that the ratio  $S_d/S_p$  measured at low particle densities ( $N/V < 10^{16} \text{ cm}^{-3}$ ) follows this prediction as the bath temperature is varied. Under high-excitation conditions, however, the ratio  $S_d/S_p$  is found to increase with density, as expected for a degenerate gas, in which particles pile up near  $k=0$ . Figure 4(c) shows this effect. Simple heating of a classical gas at high excitation level would produce an  $S_d/S_p$  ratio which would decrease, not increase, with laser power.

The above observation that  $n=CT^{3/2}$  over an order of magnitude in density is a clear indication of the quantum

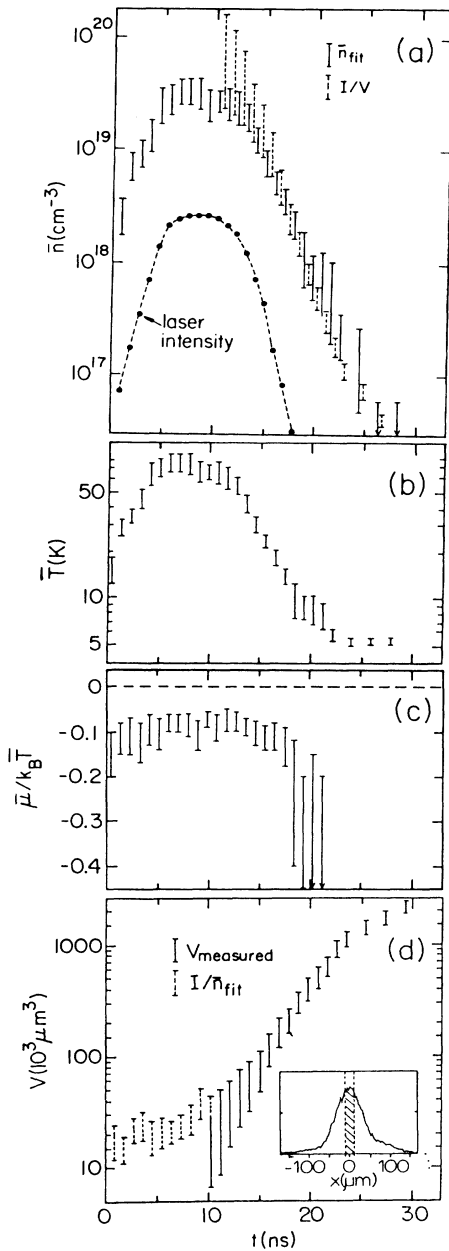


FIG. 2. (a) Density vs time for the exciton gas in  $\text{Cu}_2\text{O}$  under the same conditions as in Fig. 1. The  $n_{\text{fit}}$  bars are densities deduced from fits like those shown in Fig. 1. The  $I/V$  bars are densities deduced from measurements of total integrated luminescence intensity  $I$  and volume  $V$ .  $I$  is multiplied by an overall constant to match the density at 15 ns. (b) Excitonic gas temperature vs time, as derived from the spectral data. (c) Time variation of  $\bar{\mu}/k_B\bar{T}$  derived from the spectral fits. It remains nearly constant during the laser pulse, despite large variations in the gas temperature and density. This average  $\bar{\mu}$  derived from the spectra is expected to be slightly less than zero (as observed) because of spatial inhomogeneity of the gas density. (See text.) (d) Time variation of gas volume, as measured from spatial profiles of the luminescence. Volume is deduced for early times from  $n_{\text{fit}}$  and  $I$ , with the same overall

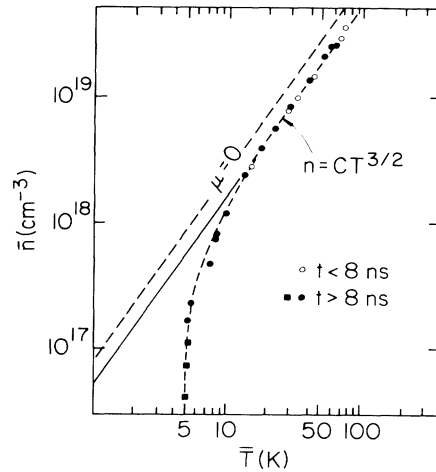


FIG. 3. Density vs temperature from the data of Fig. 2, showing Bose-Einstein saturation of the exciton gas. Circles are densities deduced from spectral fits at 1-ns intervals, where density is increasing for  $t < 8$  ns and decreasing for  $t > 8$  ns. Squares are densities deduced from  $I/V$ .

saturation condition, Eq. (1). Some condensation of excitons into the  $k=0$  state may in fact be occurring, although not in sufficient numbers to be observed in the spectra. The spectral fit value of  $\bar{\mu}/k_B\bar{T} \cong -0.1$  indicates that the surface value of  $\mu/k_B T$  is close to zero. To estimate this effect we have calculated the spatially integrated spectrum from an exponentially decreasing density,  $n(x) = n_c \exp(-x/l)$ . The calculated spectra are well fitted by a homogeneous distribution with  $\bar{\mu} = -0.1 k_B T$ , suggesting that the highest local density in the gas is indeed the critical density,  $n_c$ . Nevertheless, no conclusive evidence (e.g., a spike at  $k=0$ ) is found in these spectroscopic data.<sup>10</sup>

Why is no condensate apparent? Several factors may act to limit the  $k=0$  population and cause the system to follow the BEC phase boundary. We note that the system here differs from the textbook case in that neither the temperature nor the volume is fixed. It is well established in both metals and semiconductors that the electronic (excitonic) temperature  $T_e$  may differ from the lattice temperature  $T_{\text{lattice}}$ , because of incomplete thermalization of the carriers with respect to the lattice. At any time during the laser pulse, the excess temperature  $T_e - T_{\text{lattice}}$  is determined by the balance between the rate of heating (from the excess energy per incident laser photon) and the rate of cooling via phonon emission. Compared to a classical gas, a degenerate system

multiplier for  $I$  used in (a). These data correspond to a laser excitation area of  $\approx (30 \mu\text{m})^2$  and an orthoexciton drift length of 5–10  $\mu\text{m}$  at early times. Inset: Spatial profile of the luminescence at  $t=15$  ns. Shaded area indicates spatial resolution of the system.

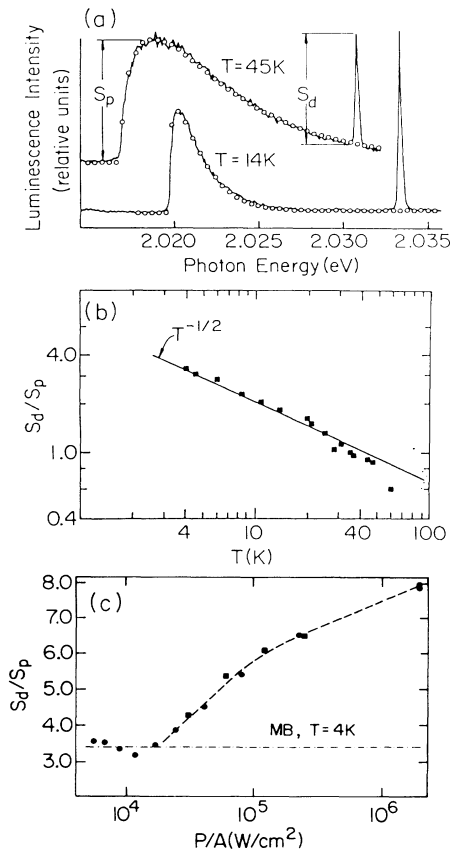


FIG. 4. (a) Orthoexcitation luminescence spectra for two temperatures under very low-power cw laser excitation. Open circles are the fit by a Maxwell-Boltzmann distribution with the given temperatures. (b) Ratio  $S_d/S_p$  plotted as a function of  $T$  for Maxwell-Boltzmann spectra like those shown in (a). (c) Time-averaged  $S_d/S_p$  plotted vs absorbed laser power  $P$  per area  $A$  for cavity-dumped  $\text{Ar}^+$  excitation.

has a much larger fraction of particles very near  $k=0$  (see Fig. 1). The exciton-phonon interaction time is larger for particles with low momentum, leading to an overall decrease in the rate of excitonic cooling as  $n$  approaches  $n_c$ , thereby increasing the instantaneous equilibrium temperature. An additional mechanism acting in the same direction is the enhanced direct radiative recombination of excitons, as noted above, which provides selective removal of cold particles at  $k=k_{\text{photon}}$  and tends to raise the gas temperature. Still another factor comes from the gradient in the chemical potential, which acts as an expansive force on the particles in the region of high gas density. Finally, a basic consideration is the

time required to establish Bose-Einstein condensation.<sup>11</sup> Our experiments may imply that this time is longer than the characteristic time scale of the experiment, about 10 ns.

Further progress in understanding of the dynamics of this system will require a detailed examination of the exciton-phonon and exciton-exciton interactions, as well as the transport and recombination properties of this unusual quantum gas. In turn, this may provide more direct information about the rate and conditions for Einstein condensation.

We are grateful to D. P. Trauernicht for his valuable advice and technical assistance. Support for this work was provided by the U.S. Air Force Office of Scientific Research Grant No. 84-0384 and National Science Foundation Grants No. DMR-85-21444, with Materials Research Laboratory support under Grant No. NSF-DMR-83-16981. We acknowledge a NATO travel grant. We thank P. J. Dunn and the Smithsonian Institution for giving us a naturally grown crystal of  $\text{Cu}_2\text{O}$ .

<sup>1</sup>A. Einstein, *Absitz. Pr. Akad. Wiss. Berlin Kl. Phys. Math.* **22**, 261 (1924).

<sup>2</sup>A. Mysyrowicz, *J. Phys. (Paris)* **41**, Suppl. 7, 281 (1980).

<sup>3</sup>C. Comte and P. Nozières, *J. Phys. (Paris)* **43**, 1069, 1083 (1982).

<sup>4</sup>E. Hanamura and H. Haug, *Phys. Rep.* **33**, 209 (1977).

<sup>5</sup>V. B. Timofeev *et al.*, in *Proceedings of the Sixteenth International Conference on Physics of Semiconductors, Montpellier, France, 1982*, edited by M. Averous (North-Holland, Amsterdam, 1983), p. 327.

<sup>6</sup>N. Peyghambarian, L. L. Chase, and A. Mysyrowicz, *Phys. Rev. B* **27**, 2325 (1983).

<sup>7</sup>D. Hulin, A. Mysyrowicz, and C. Benoît à la Guillaume, *Phys. Rev. Lett.* **45**, 1970 (1980).

<sup>8</sup>N. Caswell, J. S. Weiner, and P. Y. Yu, *Solid State Commun.* **40**, 843 (1981).

<sup>9</sup>We find that a sum of Bose-Einstein distribution functions over a range of  $\mu$  and  $T$  is approximated quite well by a homogeneous distribution with single values of  $\mu$  and  $T$ , and that the single best-fit values are close to the spatial averages of these parameters.

<sup>10</sup>One notable feature of the spectra, however, is the appearance of a low-energy tail, with a width up to 2 Å. Such a tail is expected from interparticle interactions in a dense Bose gas. H. Haug and H. H. Kranz, *Z. Phys. B* **53**, 153 (1983), have noted that a low-energy tail is expected for long-range condensate interactions.

<sup>11</sup>E. Levich and V. Yakhot, *Phys. Rev. B* **15**, 243 (1977), and *J. Phys. A* **11**, 2237 (1978).